Supplemental Document

Biomedical Optics EXPRESS

High-resolution light-field microscopy with patterned illumination: supplement

Depeng Wang,[1,3] Suva Roy,[2] Andra M. Rudzite,[2] Greg D. Field,[2] and Yiyang Gong[1,2,4]

[1]*Department of Biomedical Engineering, Duke University, Durham, NC 27708, USA*
[2]*Department of Neurobiology, Duke University, Durham, NC 27708, USA*
[3]*depeng.wang@duke.edu*
[4]*yiyang.gong@duke.edu*

This supplement published with The Optical Society on 8 June 2021 by The Authors under the terms of the Creative Commons Attribution 4.0 License in the format provided by the authors and unedited. Further distribution of this work must maintain attribution to the author(s) and the published article's title, journal citation, and DOI.

Supplement DOI: https://doi.org/10.6084/m9.figshare.14713848

Parent Article DOI: https://doi.org/10.1364/BOE.425742

High-resolution light-field microscopy with patterned illumination

DEPENG WANG,[1,*] SUVA ROY,[2] ANDRA M. RUDZITE,[2] GREG D. FIELD,[2] AND YIYANG GONG[1,2,]**

[1]*Department of Biomedical Engineering, Duke University, Durham, NC 27708, USA*
[2]*Department of Neurobiology, Duke University, Durham, NC, 27708, USA*
[*]*depeng.wang@duke.edu*
[**] *yiyang.gong@duke.edu*

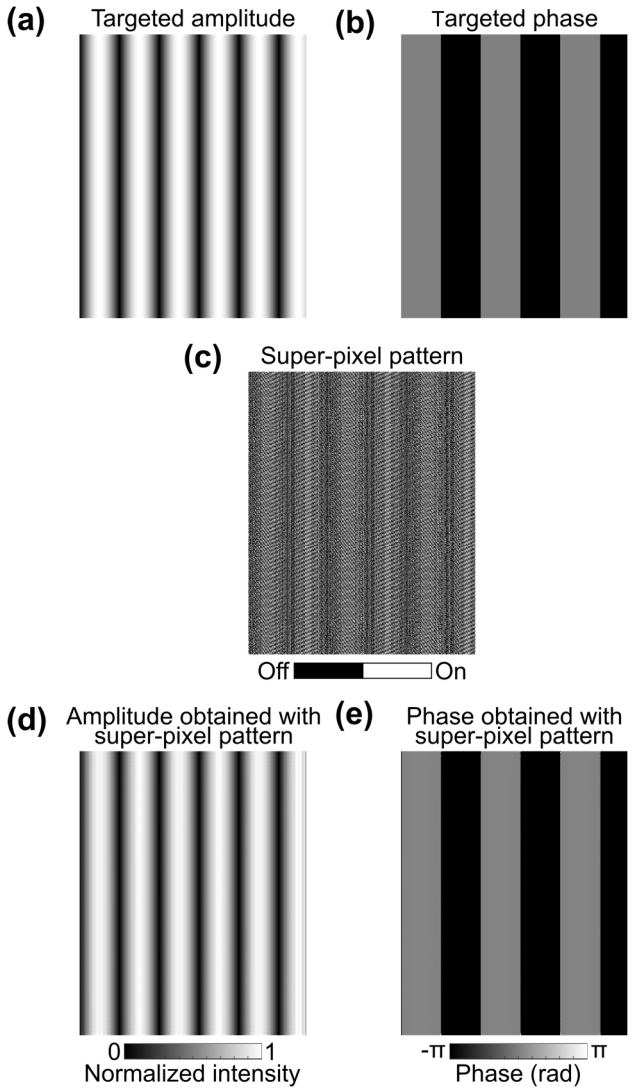

Fig. S1 – The super-pixel algorithm attempted to generate (a) the targeted amplitude and (b) the targeted phase in the Fourier plane of the optical system. The calculated (c) DMD pattern produced an (d) amplitude and (e) phase profile at the sample plane that closely matched the targeted amplitude and targeted phase, respectively.

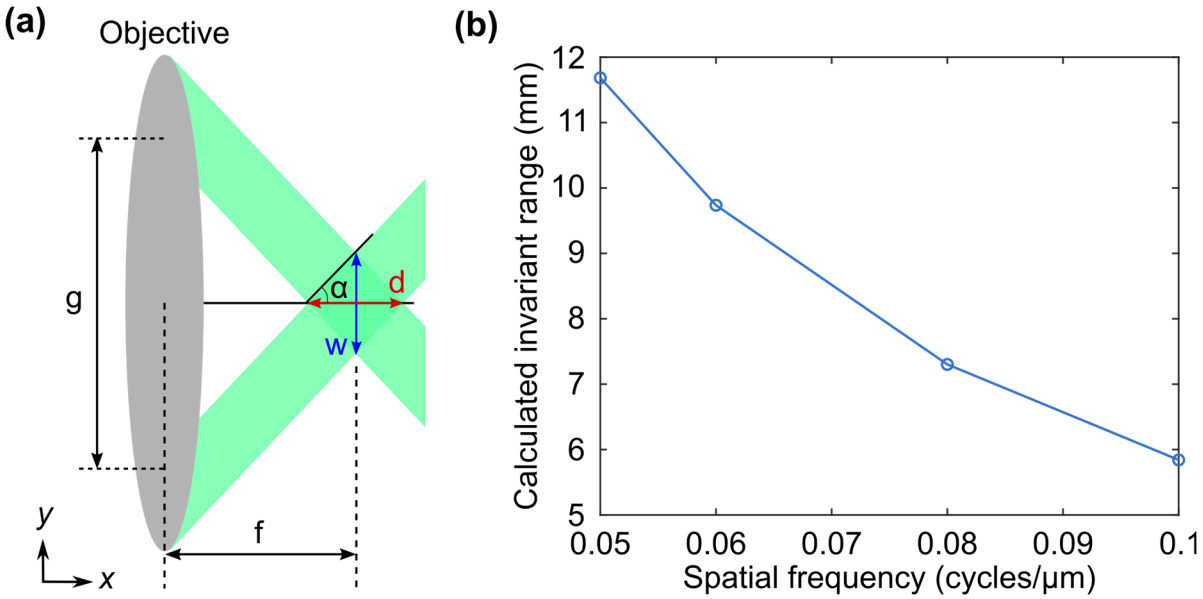

Fig. S2 – The interference between the two plane waves produced the 3D pattern for imaging. (a) The schematic drawing shows the interference between two beams of plane waves. (b) The theoretical invariant depth decreased as the spatial frequency of the grating pattern increased.

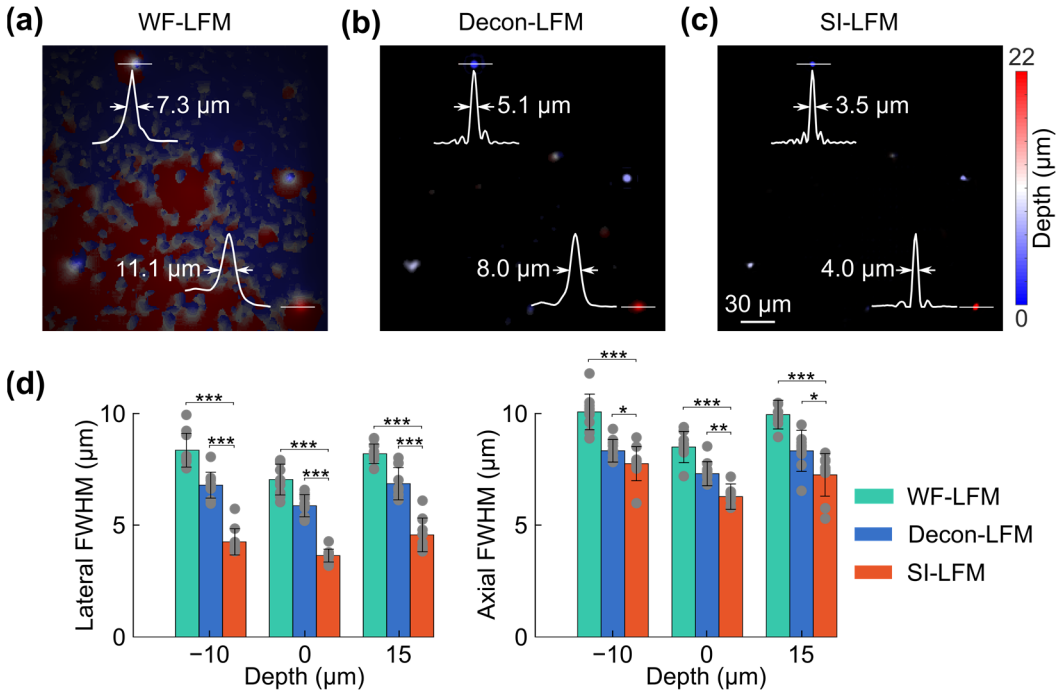

Fig. S3 – SI-LFM imaged beads over a 3D volume with better resolution than the other two modalities. (a-c) Beads within depth-encoded color images acquired by (a) WF-LFM and b Decon-LFM were larger than bead spots within the image acquired by (c) SI-LFM. All depths were referenced to the principal focal plane at $z = 0$ μm. The inset white curves are the intensity profiles of example beads, along with their FWHMs marked by the arrows. (d) The lateral and axial FWHMs of beads over different depths in a 3D sample imaged by SI-LFM were significantly smaller than the corresponding FWHMs of beads imaged by WF-LFM and Decon-LFM (dots are individual data values; error bars are standard deviations; ***$p < 0.001$, **$p < 0.01$, *$p < 0.05$, $n = 10$, two-sided Wilcoxon rank-sum test).

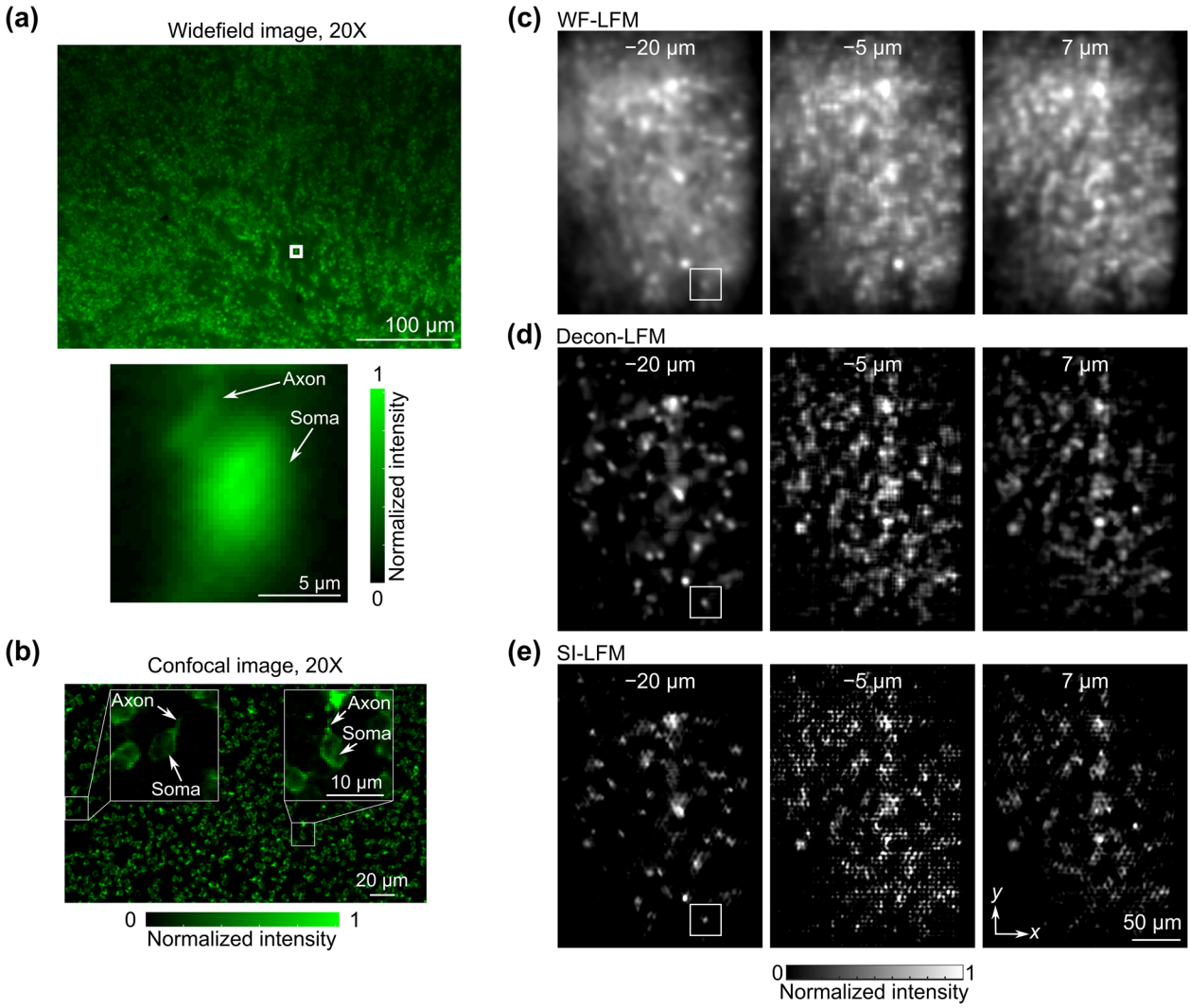

Fig. S4 – We confirmed the expression of the GCaMP6f in retina with conventional microscopy. (a) We acquired a wide-field microscopy image (*top*) at 20× with a commercial microscope (IX 50, Olympus) using a 20×/0.4NA (LCPlanFl, Olympus) objective. The excitation path used a 480/30 bandpass filter (AT480/30x, Chroma) and the emission path used a 496 nm long-pass emission filter (FF01-496/LP, Semrock). A 505 nm long pass dichroic mirror (T505lpxr, Chroma) separated the excitation light from the emission light. A zoomed-in view (*bottom*) into the white box of the top image shows a retina cell and its axonal projection. (b) We also acquired an image from a similar, but independent sample at 20× with a confocal microscope (Nikon Eclipse Ti2 inverted microscope). (c) WF-LFM produced noisy three-dimensional images and all representative layers contained substantial background. (d) Decon-LFM suppressed the background noise and clearly showed individual somas. (e) SI-LFM further improved the lateral resolution and revealed sub-cellular structures.

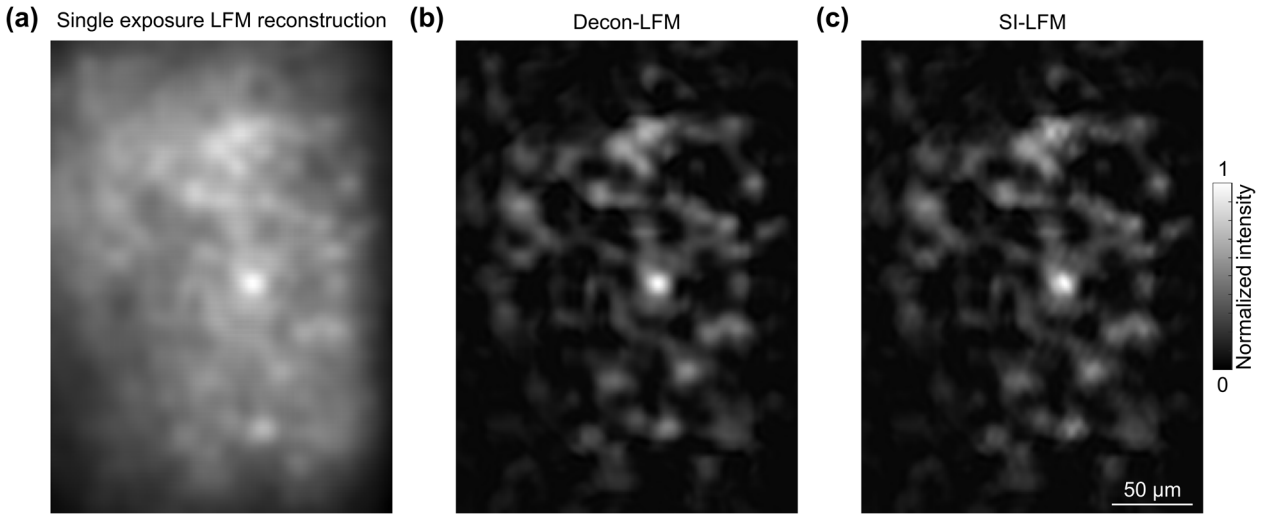

Fig. S5 – The strong scattering of a densely labeled retina sample prevented SI light-field from imaging deep into the sample. At 35 µm below the principal focal plane, the grating pattern was not visible in the (a) reconstructed image of LFM. (b) Decon-LFM and (c) SI-LFM images resulting from these source LFM images produced a similar qualitative result.

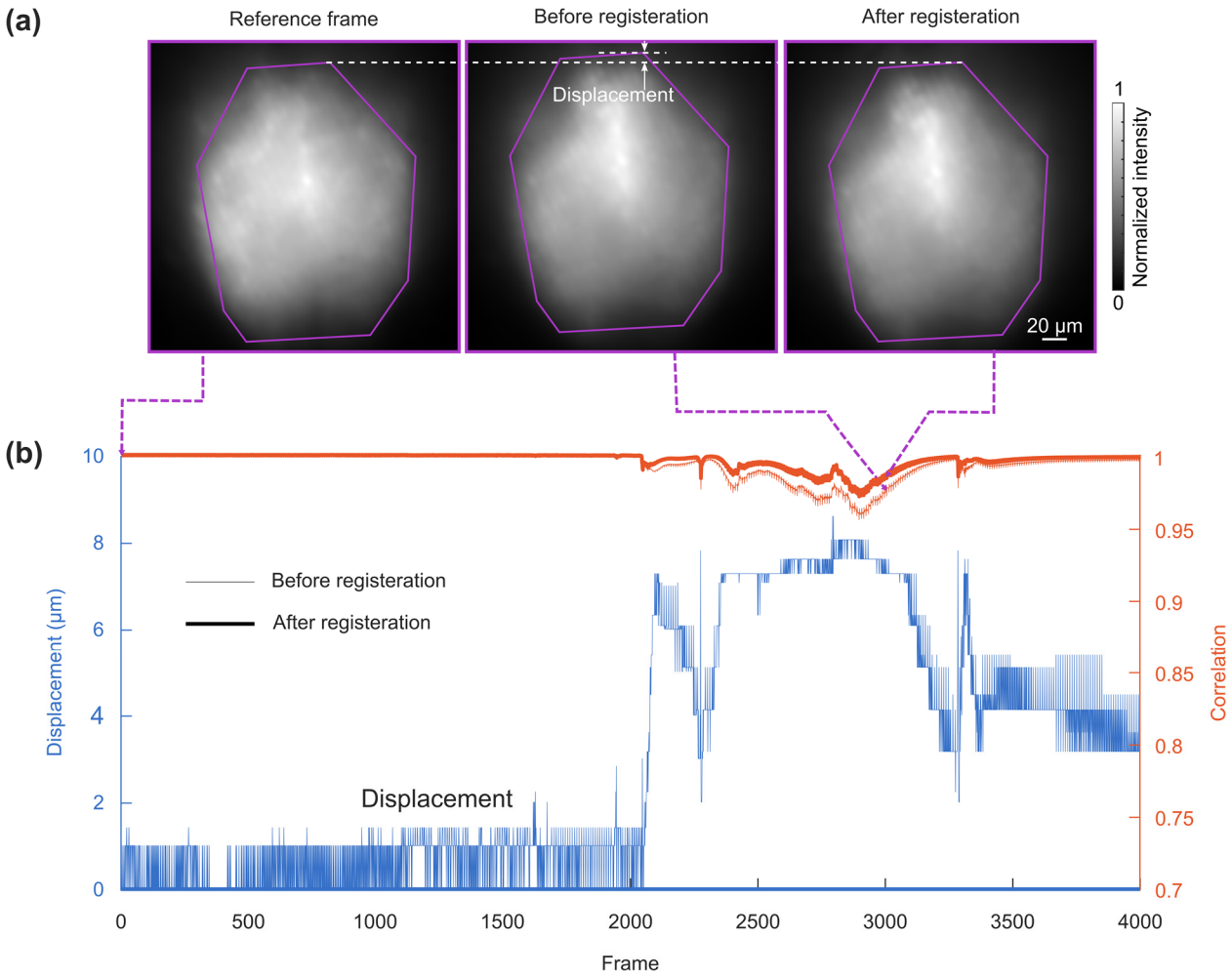

Fig. S6 – Registration aligned all frames to the reference frame and reduced fish motion. (a) Examples show the reference frame, and frames before and after registration. The boxes show the position of the imaged fish. The dashed lines serve as guides to demonstrate the corrected vertical displacement. (b) We registered all frames to the first frame (Reference frame). The registered frames showed much less displacement and higher correlation when compared with non-registered frames. We computed the displacement between frames using a block matching method and the displacement for the registered frames is zero. We also computed the correlation between the reference frame and all other frames, and the registered frames show higher correlation than non-registered frames.

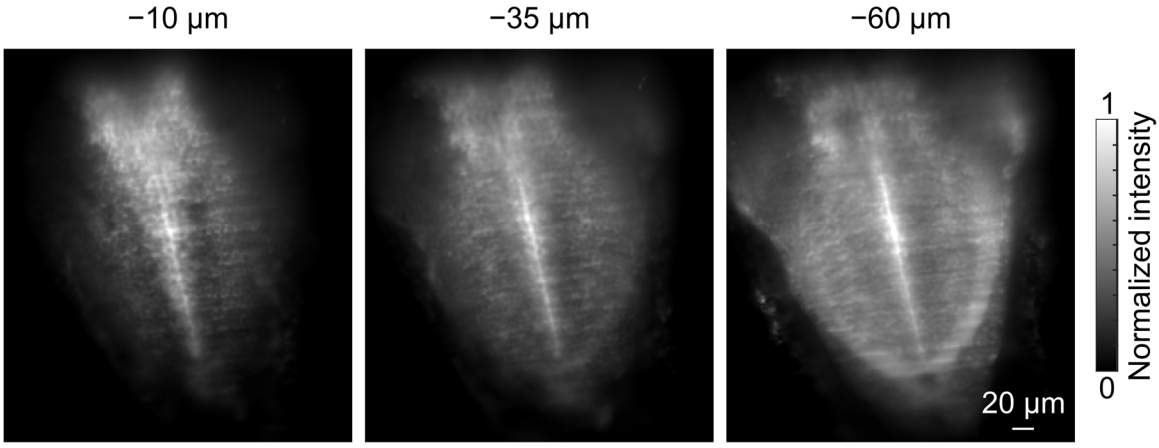

Fig. S7 – The images of zebrafish hindbrain captured by light-sheet microscopy, especially in the dorsal region, provided similar results as SI-LFM.